

# An investigation of potential regional and local source regions affecting fine particulate matter concentrations in Delhi, India

Saikat Ghosh,<sup>1</sup> Jhumoor Biswas,<sup>2,\*</sup> Sarath Guttikunda,<sup>3</sup> Soma Roychowdhury,<sup>2</sup> and Mugdha Nayak<sup>4</sup>

<sup>1</sup>Air Quality Center, Ohio University, Athens, OH, USA

<sup>2</sup>Indian Institute of Social Welfare and Business Management, Kolkata, India

<sup>3</sup>Desert Research Institute, Reno, NV, USA

<sup>4</sup>Ansal Institute of Technology, Gurgaon, India

\*Please address correspondence to: Jhumoor Biswas, Indian Institute of Social Welfare and Business Management, College Square West, Kolkata 700073, India; e-mail: [jhumoorb@yahoo.com](mailto:jhumoorb@yahoo.com)

*In this study, potential regional and local sources influencing PM<sub>2.5</sub> (particulate matter with an aerodynamic diameter >2.5 μm) concentrations in Delhi, India, are identified and their possible impact evaluated through diverse approaches based on study of variability of synoptic and local airflow patterns that transport aerosol concentrations from these emission sources to an urban receptor site in Delhi, India. Trajectory clustering of 72-hr and 48-hr back trajectories simulated at arrival heights of 500 m and 100 m, respectively, every hour for representative years 2008–2010 are used to assess the relative influence of long-distance, regional, and subregional sources on this site. Nonparametric statistical procedures are employed on trajectory clusters to better delineate various distinct regional pollutant source regions. Trajectory clustering and concentration-weighted trajectory (CWT) analyses indicate that regional and subregional PM<sub>2.5</sub> emission sources in neighboring country of Pakistan and adjacent states of Punjab, Haryana, and Uttar Pradesh contribute significantly to the total surplus of aerosol concentrations in the Delhi region. Conditional probability function and Bayesian approach used to identify local source regions have established substantial influence from highly urbanized satellite towns located southwest (above 25%) and southeast (above 45%) of receptor location. There is significant seasonal variability in synoptic and local air circulation patterns, which is discerned in variability in seasonal concentrations. Mean of daily averaged PM<sub>2.5</sub> concentrations at the Income Tax Office (ITO) receptor site over Delhi at 95% confidence level is highest in winter, ranging between 209 and 185 μg m<sup>-3</sup> for the entire study period. The annual variability in air transport pathways is more in winter than in other seasons. Year-to-year variability is present in aerosol concentrations, especially during winter, with standard deviations varying from a minimum of 60 μg m<sup>-3</sup> in winter 2009 to a maximum of 109 μg m<sup>-3</sup> in winter 2010.*

*Implications:* The rapid urban development of Delhi, capital of India, has resulted in increased concentrations of aerosols, which far exceed National Ambient Air Quality Standards making Delhi one of the worst polluted areas. Hence, the region demands development of appropriate emission control strategies that minimize the air quality impacts. This paper addresses the impacts of transboundary air pollutants and local emissions on Delhi's air quality and reveals the influence of air circulation patterns on aerosol concentrations. These factors must be considered in designing of effective emission reduction strategies in Delhi region.

## Introduction

Elevated levels of fine particulate matter (PM<sub>2.5</sub>; with aerodynamic diameter less than 2.5 μm) contribute to detrimental health effects (Health Effects Institute [HEI], 2010a, 2010b; Pope et al., 2011) and reduced visibility in urban centers. Aerosols also influence climate change through radiative forcing (Shindell and Faluvegi, 2009; Shindell et al., 2012). Aerosol concentrations are influenced not only by in situ formation but also through transport affected by prevailing meteorological conditions. Hence, several past studies (Ketzler and Berkowicz, 2005; O'Connor et al., 2008) have investigated the source and fate of aerosols.

Delhi, capital of India (28°4'N, 77°2'E), is a megacity located in central India, covering an area of 1483 km<sup>2</sup> with population of more than 16 million. The rapid urbanization has accentuated environmental stress, resulting in rise in atmospheric concentration levels of air pollutants, which pose serious public health risks for sensitive population in Delhi (Pandey et al., 2005; Guttikunda and Goel, 2013). Efforts have been instigated in the greatly urbanized Delhi region (Mitra and Sharma, 2002; Srivastava and Jain, 2007; Tiwari et al., 2013) to monitor and analyze the aerosol concentrations and to comprehend the dynamics of their emissions, formation, travel, and removal. However, the continual high concentrations of PM<sub>2.5</sub> in Delhi (Guttikunda, 2009; Biswas

et al., 2011) despite implementation of emission control measures (Khairwal et al., 2006) are of great concern to relevant stakeholders. Scientific investigations have confirmed that aerosol concentrations remain high throughout the year in Delhi (Mohan and Payra, 2009; Srivastava et al., 2012), exceeding national ambient air quality standards (Sharma et al., 2013), and this situation may still continue in the future, even into 2030, unless appropriate emission controls are developed (Dholakia et al., 2013). Sources of particulates comprise various types of combustion, including motor vehicles and road dust (local sources), power plants (local and regional sources), residential wood burning, agriculture burning, and some industrial processes (local and regional sources) (Guttikunda and Calori, 2013; Li et al., 2014). Particles form and grow by mechanisms of condensation, coagulation, and nucleation, and thereafter, atmospheric chemical and physical processes deposit them. Aerosols undertake long-range transport, primarily through episodic events associated with biomass burning plumes, dust storms, and fast transport of industrial pollution (National Research Council [NRC], 2010). The source contribution largely depends on the atmospheric thermodynamics and synoptic-scale, meso-scale, and local circulation patterns (Zhang and Wexler, 2008; Buseck and Schwartz, 2014). It is thus important to identify the characteristic spatial and temporal scales to demarcate local, regional, and continental sources and estimate their potential impact. This will aid in development of effectual pollution control strategies for the Delhi region.

Air mass trajectories have been effectively used in this regard, and cluster analysis of the trajectories has proved to better delineate specific meteorological scenarios and distinct common transport patterns associated with high pollutant concentrations at different locations (Salvador et al., 2008; Markou and Kassomenos, 2010; Chuang et al., 2014). Back-trajectory analyses in India have been utilized in investigations of origin of ionic and biogenic constituents in precipitation (Norman et al., 2001; Budhavant et al., 2014). Some other studies have applied trajectory simulations with aerosol optical depth (AOD) data. Five-day trajectories have been employed during days with low and high AOD values observed in Dehradun, northern India (Rana et al., 2009). The study has determined that aerosol sources are initiated from west in central Asia during March and from east and southeast in the Indo-Gangetic plain during winter. Air masses from Delhi have been traced to travel from Indian Ocean via semiarid and arid regions in Oman, Pakistan, and India (Gupta et al., 2006). Cluster analysis and concentration-weighted trajectory (CWT) analysis have illustrated potential sources of high aerosol loading in Dibrugarh located in northeast India from west Asia and the Indo-Gangetic plain during winter and premonsoon seasons, respectively (Gogoi et al., 2010). Although forward-trajectory calculations have been used to assess impact of outward transport of emissions from the Delhi region (Gurjar et al., 2005), there has been a dearth of studies on comprehensive assessment of transportation paths of particulate matter into the Delhi region.

This study aims to identify and develop a perspective on the relative importance of transboundary flux of  $PM_{2.5}$  and local emissions and provide a representation of subcontinental,

regional, and local sources affecting air quality in Delhi. Characterization of particulate matter has shown strong influence of local sources (vehicular, local industrial processes and roadside dust) (Singh et al., 2011). A recent study (Gupta and Mohan, 2013) has, however, established the significance of contribution of long-distance sources towards particulate matter episodes over Delhi. In this study, flow routes of air parcels to an urban site in Delhi from regional and remote continental sources have been determined through back-trajectory analyses and subsequent clustering. Besides the source regions where the trajectories originate, there are several other factors, such as the presence of emission sources along the air mass trajectory, the time it takes for the air mass to reach the receptor, and the height of air mass when it approaches the receptor, that also decide the impact on local air quality (Miller et al., 2010). Concentration-weighted trajectory (CWT) approach (Cheng et al., 2013) has been applied to address potential regional sources of contribution and determine the characteristic spatial and temporal scales involved in  $PM_{2.5}$  transport to this region. The study has been conducted over a period of 3 yr to ascertain seasonal and interannual variations in airflow transport patterns and their consequent impact on the variability in fine particulate matter concentrations over Delhi. To characterize potential local sources, an analysis of wind directions associated with high  $PM_{2.5}$  concentrations has been conducted using conditional probability and Bayesian probability methods.

## Data Collection

Income Tax Office (ITO) (latitude 28.628°, and longitude 77.241°), located in the commercial zone of Delhi, is adjacent to one of the busiest traffic junctions (Figure 1). For the modeling simulations, hourly observations for fine particulate matter have been retrieved from the ITO site for the years 2008–2010. The local sources of pollution at this site are mostly road transport and road dust (Guttikunda and Calori, 2013). The monitoring site has been set up and is maintained by the central environmental regulatory body Central Pollution Control Board (CPCB) under the National Air Quality Monitoring Program (<http://cpcb.nic.in>; CPCB, 2014). The meteorological data used in the model are the National Centers for Environmental Prediction (NCEP) Global Data Assimilation System (GDAS) (3-hourly, 1° resolution) archived data.

The Regional Emissions Inventory in Asia (REAS) version 2.1 for  $PM_{2.5}$  species for base year 2008 has been used to corroborate major regional emission source regions identified by trajectory clusters and CWT. The gridded emission inventory is at  $0.25^\circ \times 0.25^\circ$  grid resolution. Growth factors for REAS version 2.1 are under development (Kurokawa and Ohara, 2014). Details of the emission inventory are specified in (Krakow et al., 2013). In this study, total  $PM_{2.5}$  emissions from all sectors except power plants have been merged and averaged for each season for 2008. The power point emissions have been allocated separately on individual grid cells based on latitude and longitude. Consequently, the concentration-



Figure 1. ITO site at Delhi.

weighted trajectory values and REAS emissions have been collocated to understand the colinearity amongst the estimated weighted grid values and emissions.

## General Meteorology

Delhi is located almost entirely on the Indo-Gangetic plain in a semiarid climate zone, with long summers and extremely foggy winters (Guttikunda and Gurjar, 2012). The isoclines and wind vectors have been plotted at 850 mb for three representative days for each of the three seasons: for winter, January 15, 9:00 a.m.; for summer, May 15, 9:00 a.m.; and for monsoon, September 15, 9:00 a.m. (Figure 2). As illustrated in the maps, the synoptic patterns exhibit seasonal changes, with relatively moderate northwesterly wind patterns dominating winter season and moderate to strong southwesterlies predominant in summer. The monsoon synoptic wind pattern is a mix of moderately strong

northwesterlies, westerlies, and southwesterlies. In winter, the synoptic patterns feature more stagnant conditions due to shallow mixed layer caused by inversion, resulting in poor ventilation within mixed layer. This results in foggy conditions and extreme accumulation of aerosol concentrations in Delhi. The back trajectories simulated in this study are in accordance with general airflow over the region.

## Methodology

### HYSPLIT model

The trajectories have been generated from wind-field and pressure data using National Oceanic and Atmospheric Administration's (NOAA) Hybrid Single Particle Lagrangian Integrated Trajectory (HYSPLIT) version 4 (Draxler and Hess, 1998) modeling system. The PC-based HYSPLIT has been

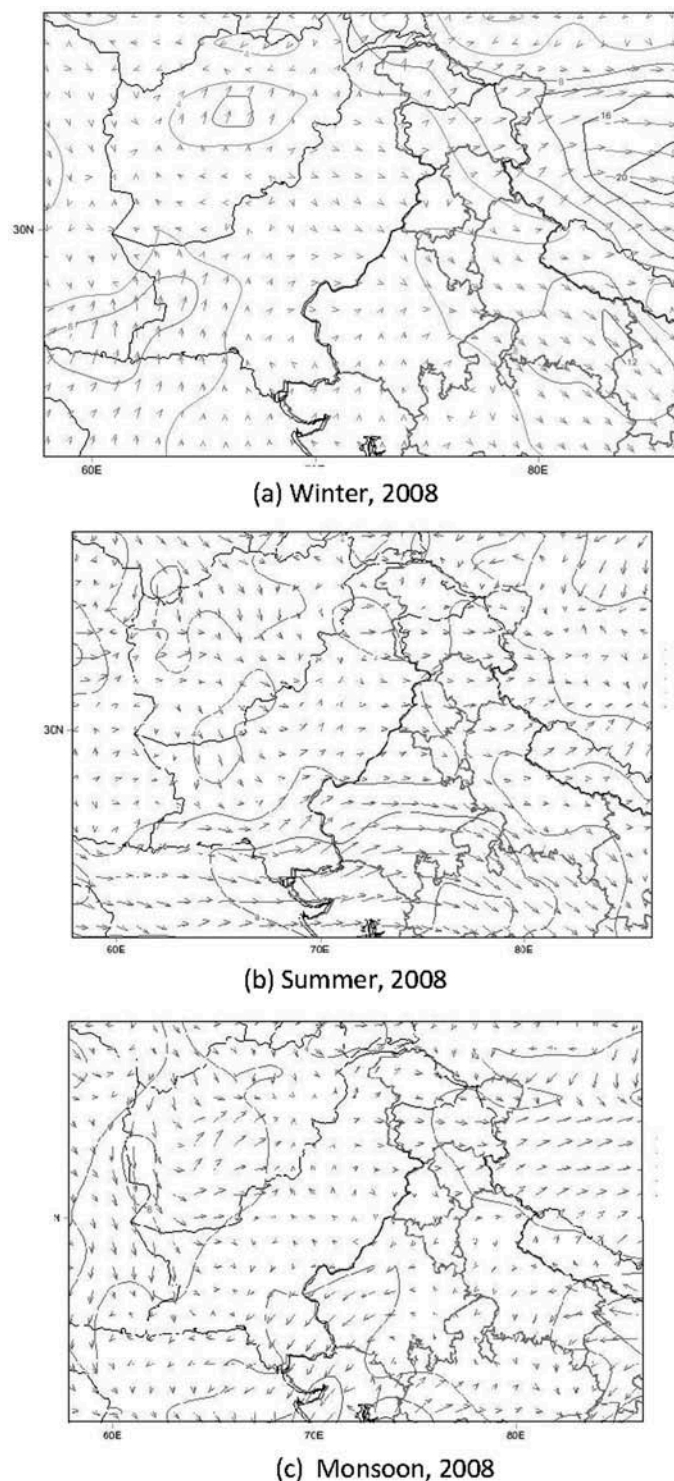


Figure 2. Air mass trajectory analysis.

employed to simulate 72-hr and 48-hr trajectories (backward normal mode) for 500 m and 100 m arrival heights, respectively, to attempt to differentiate relative importance of long-distance versus regional emission sources. The model has been

run with tel script looping through starting times every hour. These back trajectories have been linked to the hourly concentrations at the ITO sampling site with corresponding starting times for generating clusters.

The three-dimensional backward trajectories impart Lagrangian path of air parcels, which have been used to distinguish potential source regions and transport pathways of pollutants. To assess seasonal and interannual variability, the modeling simulations have been conducted over three seasons. To maintain data parity, a period of 4 months has been considered for each season, summer (March–June), monsoon (July–October), and winter (November–December, January–February), that covers a mix of pre- and post-seasonal effects for each of the three years (2008–2010). Details of seasonality in Delhi have been expounded in (Guttikunda and Gurjar, 2012).

### Trajectory clustering

To detect synoptic and meso-scale circulation patterns, a clustering technique is applied. The trajectories are clustered according to their proximities using k-means clustering technique in homogeneous groups based on least total within-cluster spatial variance. Cluster analysis is a multivariate statistical analysis tool applied on a large number of individual trajectories calculated every day. Clustering techniques enable us to reduce intrinsic errors due to uncertainties in meteorological data, simplified underlying model assumptions and numerical analyses by averaging out the errors on individual trajectories generated (Stohl et al., 2002). The number of clusters is reduced by merging clusters whose average trajectories are closest and retaining only those clusters that are noticeably different in wind speeds and wind direction. Clustering has been done using open air clustering algorithm (Carslaw and Ropkins, 2012) based on geographic dissimilarity of Euclidean distance (<http://www.openair-project.org/>) for each season and year. The clusters represent distinct transport patterns and originate from different potential source regions. The groups of trajectories within each cluster have been mapped with the corresponding  $PM_{2.5}$  concentrations.

### Statistical tests

To test the significance of the intercluster variation in median, nonparametric statistical tests such as Kruskal-Wallis and Mann-Whitney (Daniel, 1978) have been employed. The Kruskal-Wallis test is a commonly used nonparametric technique for testing the null hypothesis that several samples have been drawn from the same population. It is used if the population distributions are non-normal. A parametric test based on analysis of variance (ANOVA) is carried out for the same purpose when the samples have come from normal populations. Kolmogorov-Smirnov test is performed to identify if the population distributions are normal. If not (i.e., if the P values of the test are less than 0.05), which happened in this case, then the Kruskal-Wallis test can be performed. In this case, the Kruskal-Wallis test (applied to three or more clusters) leads to the rejection of the null hypothesis of equality, and the conclusion is that not all the clusters under consideration are identical in

respect of their medians. To distinguish which of the two clusters are significantly different, it may be appropriate to use a two-sample test and perform pairwise comparisons. The Mann-Whitney test has been used to examine whether the median concentrations across the selected independent random clusters are significantly different. The two techniques have been used in combination to further decrease the number of individual clusters and hence reduce the redundancy of similar sources.

### Concentration-weighted trajectory (CWT) for assessment of regional sources

To understand the spatial distribution of potential source regions and their relative significance, concentration-weighted trajectory (CWT) method (Han et al., 2007) is used to calculate the trajectory weighted concentrations. To calculate CWT, the whole geographic region covered by the trajectories is divided into an array of grid cells whose size is dependent on the geographical scale of the trajectories. The CWT method assigns the concentration values at the receptor site to estimate the trajectory weighted concentration in each grid cell by averaging the sample pollutant concentrations that have associated trajectories crossing each grid cell, as given in eq 1 below:

$$\bar{C}_{ij} = \frac{1}{\sum_{k=1}^N \tau_{ijk}} \times \sum_{k=1}^N \{c_k \times \tau_{ijk}\}, \quad (1)$$

where  $\bar{C}_{ij}$  is the average weighted concentration in the  $(i, j)$ th cell,  $k$  is the index of the trajectory,  $c_k$  is the pollutant concentration measured on the arrival of trajectory  $k$ ,  $N$  is the total number of trajectories, and  $\tau_{ijk}$  is the time spent in the  $(i, j)$ th cell by trajectory  $k$ . A high  $\bar{C}_{ij}$  value is associated with high pollutant concentrations at the receptor site. The concentration-weighting factor is allocated on the count of frequency of back-trajectory segment end points in grid cells. In this study, CWT concentrations have been generated from the  $PM_{2.5}$  concentrations observed on arrival of the corresponding backward trajectories. Each cell is assigned an average weighted value of the concentrations from the all the trajectories. Thus, higher CWT value of a grid cell indicates that an air parcel passing over the particular grid cell will cause high concentrations at the receptor (sampling station). CWT concentrations have been generated using TrajStat algorithm (Wang et al., 2009) at 0.25° grid resolution with southwest corner at (22°N, 64°E) and northeast corner at (34°N, 81°E).

The CWT is an advantageous methodology because it gives information on the relative significance of different potential source regions in addition to the spatial distribution of the sources (Lin et al., 2013).

### Conditional probability function (CPF) and Bayesian approach to evaluation of local source impact

For the analysis of impact of local sources, CPF has been used to represent the probability of different ranges of  $PM_{2.5}$  concentrations linked with specific wind directions. The wind directions

have been segregated into eight equal sectors between 0° and 360°. The  $PM_{2.5}$  concentrations have been analyzed from each of the eight wind directions. Lower values of CPF signify lower likelihood of the particular range of  $PM_{2.5}$  concentrations coinciding with related wind direction, whereas higher CPFs imply higher chances of alignment between specific ranges of  $PM_{2.5}$  concentrations with that particular wind sector. This helps to determine the dominant wind directions contributing to explicit ranges of  $PM_{2.5}$  concentrations at the receptor site.

The Bayesian approach has been adopted to estimate the contribution of each direction of wind towards high values of  $PM_{2.5}$  concentrations ( $>120 \mu\text{g m}^{-3}$ ) by evaluating posterior probabilities of different directions responsible for elevated  $PM_{2.5}$  concentrations. Higher probability values indicate more contribution from the particular associated wind direction towards  $PM_{2.5}$  concentrations at the receptor site. This type of analysis can help delineate relative influence of surrounding local sources.

## Results and Discussion

### Data characteristics

The data analysis reveals that for the three consecutive years (2008–2010), the seasonal means are  $197 \mu\text{g m}^{-3}$  in winter,  $97 \mu\text{g m}^{-3}$  in summer, and  $87 \mu\text{g m}^{-3}$  in monsoon. The range of mean of daily averaged concentrations of  $PM_{2.5}$  over Delhi at 95% confidence level is between 209 and  $185 \mu\text{g m}^{-3}$  in winter, 103 and  $92 \mu\text{g m}^{-3}$  in summer, and 97 and  $77 \mu\text{g m}^{-3}$  in monsoon for the three years. The seasonal standard deviations (SD) and ranges for three consecutive years are as follows: for winter of 2008–2010, the SD is  $95 \mu\text{g m}^{-3}$  and range is  $10\text{--}570 \mu\text{g m}^{-3}$ , for summer SD is  $48 \mu\text{g m}^{-3}$  and range is  $17\text{--}309 \mu\text{g m}^{-3}$ , and for monsoon SD is  $74 \mu\text{g m}^{-3}$  and range is  $10\text{--}372 \mu\text{g m}^{-3}$ . The highest magnitude and variability in concentrations are emphasized in winter.

The results for each season for the three successive years are displayed in Table 1. Since the mean of daily averaged concentrations exceeded the NAAQS 24-hr standard ( $60 \mu\text{g m}^{-3}$ ), almost 100% in winter season for all the three years, we have set a seasonal threshold by considering the proportion of time each season exceeded its own standard (mean across seasons for 2008–2010) to meaningfully intercompare data with similar seasonal characteristics. As revealed in Table 1, the year 2010 contributes most to the high averages in winter, followed by the year 2008. The relative contribution of the year 2009 is the lowest amongst the three years. The SD value is highest for winter of 2010, indicating maximum variability. The highest concentrations for the monsoon time period for all the three years are recorded in the postmonsoon period in the month of October. The limit of daily averaged winter  $PM_{2.5}$  concentrations for the winter period of 2008–2010 has been exceeded most in 2010, followed by 2008 and then 2009. The proportion of exceedance days in summer is most in 2010, followed by 2008 and thence by 2009, whereas in monsoon the exceedance days are more uniformly distributed (Table 1). The range of

**Table 1.** Summary statistics for PM<sub>2.5</sub> in  $\mu\text{g m}^{-3}$  (2008–2010)

| Statistic                                      | Winter |      |      | Summer |      |      | Monsoon |      |      |
|--|--------|------|------|--------|------|------|---------|------|------|
|  | 2008   | 2009 | 2010 | 2008   | 2009 | 2010 | 2008    | 2009 | 2010 |
| Mean   | 187    | 133  | 271  | 87     | 78   | 125  | 93      | 68   | 101  |
| Standard deviation (SD)                        | 69     | 60   | 109  | 41     | 24   | 54   | 88      | 63   | 76   |
| Days (%) exceeding mean                        | 41     | 20   | 69   | 33     | 17   | 66   | 18      | 20   | 39   |
| Days (%) exceeding mean + SD                   | 9      | 0    | 37   | 12     | 0    | 24   | 21      | 23   | 20   |
| Days (no.) of extremely high PM <sub>2.5</sub> | 1      | 0    | 5    | 1      | 0    | 6    | 9       | 5    | 14   |

variability is enunciated by exceedance of mean + SD values calculated over the three years for each season. The results are expressed in Table 1. Winter and summer of 2010 show the highest degree of variability in this regard, followed by summer and winter of 2008. The year 2009 exhibits the least variability during winter and summer, exceeding the threshold zero times. The daily monsoon averages exceed mean + SD threshold values more uniformly over the three years, caused by differences in monsoon and postmonsoon concentrations.

To detect if there is any suspect outliers (extremely high value of PM<sub>2.5</sub>) on a particular day, a statistical measure has been computed as a threshold limit value by adding 1.5 times interquartile range to the 75th percentile value for daily averaged values for each specific set of seasons across all the three years. Any value exceeding that limit is considered to be an extreme PM<sub>2.5</sub> value. The limits are  $428 \mu\text{g m}^{-3}$  in winter,  $292 \mu\text{g m}^{-3}$  in summer, and  $186 \mu\text{g m}^{-3}$  in monsoon. It is seen that this threshold is exceeded five times in winter and six times in summer for 2010, zero times in winter and summer of 2009, and once each for winter and summer of 2008. For the monsoon time period, the above limit is exceeded 14 times in 2010, 5 times in 2009, and 9 times in 2008 mostly in the month of October. The above set of analyses depicts prominent seasonal variability in 24-hr averaged PM<sub>2.5</sub> concentrations as well as pronounced interannual variability, especially in winter concentrations. High winter averages of PM<sub>2.5</sub> occur due to limited pollutant dispersion caused by formation of high pressure system over Delhi, which results in lower mixing heights with stable boundary layer. The Delhi region and its surroundings are characterized by high emissions, which have actuated high aerosol concentrations. However, the primary cause of interannual variations can be ascribed to atmospheric variability that can affect pathways of aerosols, their formation, residence time in the atmosphere, and their deposition. A study of transport pathways over state of Delhi can thus help us better comprehend the sources and movement of air pollutants and fluctuations in concentrations.

### Seasonal flow patterns at 500 m and their allied concentrations (2008–2010)

The sampling heights of 500 m is chosen for arrival at the receptor site to study the influence of synoptic air masses on the seasonal variation of surface aerosols over Delhi, whereas the 3-day time period is consistent with the residence time of

aerosols. The Kruskal-Wallis test designated significant differences in aerosol concentrations amongst the nine trajectory clusters arriving at the sampling location for each of the three years at arrival heights of 500 m and 100 m. Pairwise comparisons of clusters of PM<sub>2.5</sub> concentrations have been performed using the Mann-Whitney test to establish noteworthy differences in median concentrations across clusters to establish distinct sources.

*Winter season (2008–2010).* It is seen that for all the three years in winter (2008–2010), air pollution in the Delhi region is mainly affected by subregional and regional pollution sources (Figure 3). The transport routes and the direction of trajectories indicate that in winter the transport pathways are distributed in west, northwest, and southeast, with clusters from northwest dominating the transport pattern.

In winter of 2008, the origins of faster-moving moderate-speed clusters are spread out from northwest in Afghanistan and Pakistan (C1 + C2 + C3; consisting of 41% of ensemble of trajectories from these areas that governs regional transport), southwest from tail of Pakistan through Rajasthan (C7 with 5% trajectories), and southeast from Uttar Pradesh region (C6 with 8%), which are fewer in number (Figure 3 and Table 2). However, it is the slow-moving, shorter clusters originating from slightly west (13%) and northwest (14%) of Delhi from Punjab and Haryana and slow, short recirculating trajectory clusters around Delhi area (C4 with 19% trajectories) that play a major role in winter pollution. Estimating the percentile distribution of concentrations (Table 2), it is seen that the shorter, slow-moving clusters originating from industrial regions of Punjab, Haryana, and slightly east of Delhi have the highest mean concentrations exceeding  $200 \mu\text{g m}^{-3}$ . The interquartile distributions of these clusters consist of some of the highest values, with 75th percentile values exceeding  $270 \mu\text{g m}^{-3}$  and 95th percentile values exceeding  $380 \mu\text{g m}^{-3}$ . These are some of the highest values for winter of 2008. The trajectory clusters originating from Afghanistan, Pakistan, and Rajasthan have relatively lower means in comparison with the shorter clusters. However, their 75th and 95th percentile values are high, surpassing  $270 \mu\text{g m}^{-3}$  (Table 2). These concentrations are in range with the concentrations of the shorter clusters, showing that these moderately long-distance clusters pick up local emissions as they move towards the ITO receptor site.

The primary difference in circulation patterns of winter of 2009, which has relatively lower values in comparison with 2008 and 2010, is that long-distance transport patterns

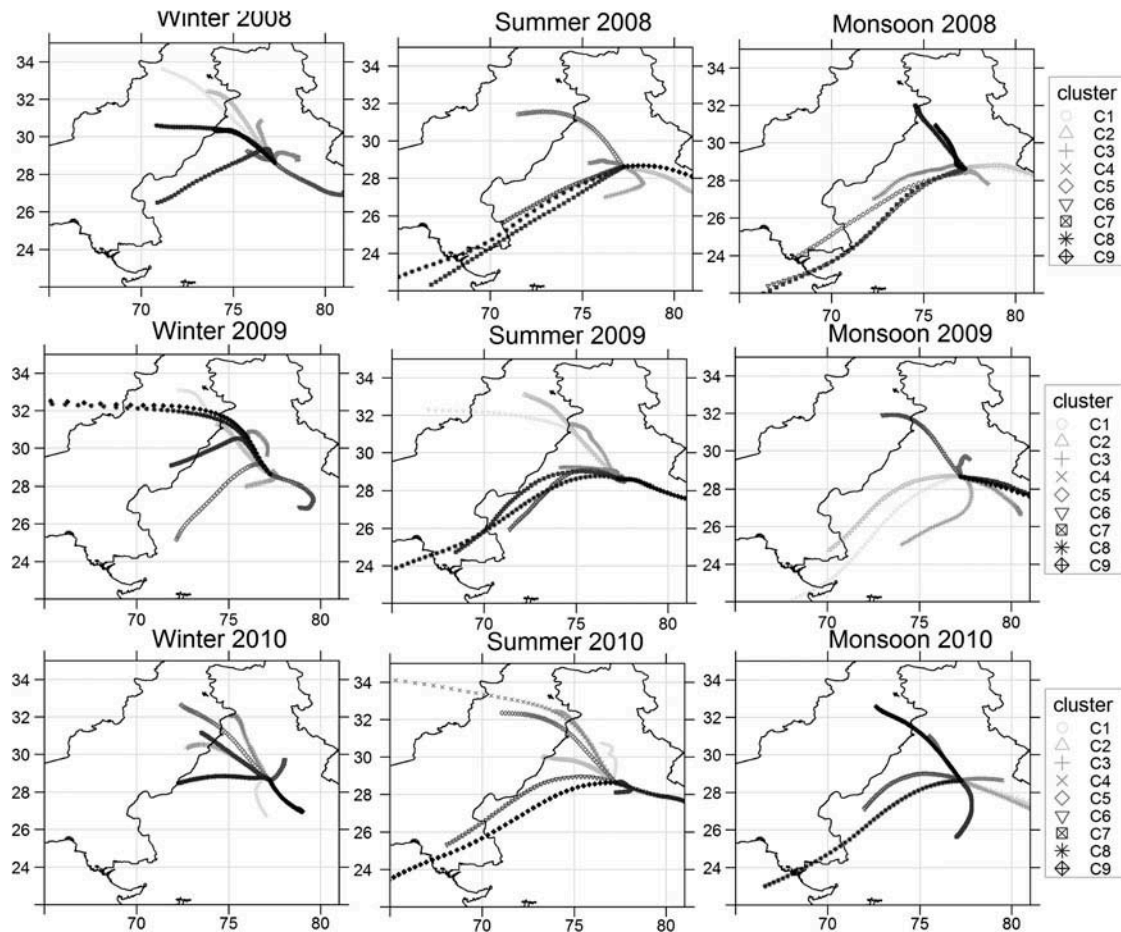


Figure 3. Trajectory clusters for different seasons, 2008–2010.

dominate. Fastest long trajectories (C8 and C9, enfolding 10% of trajectories) originate in Middle East countries such as Iran, Iraq, and Saudi Arabia and are simulated reaching Delhi from northwest in winter season of 2009. Moderately fast trajectory clusters (C1, C2, and C7) include 42% trajectories (Figure 3 and Table 2). They originate from northwest in Afghanistan, border of India and Pakistan, and southwest Karachi region of Pakistan. The importance of recirculation is exhibited with 34% trajectories, showing the importance of more local transport on this urban site. The associated concentrations with clusters from the Middle East have low seasonal averages of  $68 \mu\text{g m}^{-3}$  (Table 2). The highest concentrations are coupled with shorter, slower clusters and local recirculating clusters, with high averages exceeding  $130 \mu\text{g m}^{-3}$ . The shorter clusters C2 from northwest and C6 from southeast exhibit the highest concentrations, demonstrating the importance of regional transport. However, since the dominant synoptic patterns are more integrated with intercontinental and long-distance transport, 2009 has the lowest variability in winter concentrations amongst the three years.

The winter of 2010 has some of the highest concentrations amongst the three winters. The dominating transport patterns are slow-moving local recirculating and shorter-length regional trajectory clusters. The highest trajectory loading (52%) is in

the short, slow-moving recirculating clusters originating immediately north, northeast, and southeast regions of Delhi that pick up local emissions around Delhi area (Figure 3 and Table 2). There is no distinct intercontinental-transport pattern as in the case of 2009. The moderately fast trajectory cluster, which represents the longest distance transport in the winter of 2010, begins from northwest from industrial Lahore on border of Punjab and Pakistan, picks up high concentrations from power plant emissions over Punjab and Haryana, and finally merges with local circulation patterns in Delhi. All the trajectory clusters are associated with high mean values, ranging from 170 to  $345 \mu\text{g m}^{-3}$  and have high interquartile distributions (Table 2). Although the dominant transport patterns are similar to winter of 2008, the shorter length of the trajectory cluster ensures greater residence time in each grid cell in urban areas, enabling the air parcels to pick up higher loadings of pollutants. The winter analyses (2008–2010) illustrate the importance of synoptic, regional, and local circulations in the build-up of air pollution.

*Summer season (2008–2010).* The trajectory cluster pattern for summer season is illustrated in Figure 3 for all the years. The summer season is dominated by southwesterly flows. Fast-moving maritime transport patterns C7 and C8 (9–11% of

**Table 2.** Summary statistics of seasonal trajectory clusters for PM<sub>2.5</sub> (µg m<sup>-3</sup>), 2008–2010

| Cluster | Season | Mean |      |      | 25th Percentile |      |      | 75th Percentile |      |      | 95th Percentile |      |      | % of Trajectories |      |      |
|---------|--------|------|------|------|-----------------|------|------|-----------------|------|------|-----------------|------|------|-------------------|------|------|
|         |        | 2008 | 2009 | 2010 | 2008            | 2009 | 2010 | 2008            | 2009 | 2010 | 2008            | 2009 | 2010 | 2008              | 2009 | 2010 |
| C1      | W      | 139  | 102  | 271  | 89              | 68   | 142  | 162             | 124  | 371  | 279             | 214  | 479  | 16                | 15   | 7    |
|         | S      | 98   | 74   | 122  | 53              | 46   | 84   | 136             | 86   | 137  | 181             | 156  | 220  | 13                | 16   | 10   |
|         | M      | 35   | 41   | 47   | 29              | 16   | 29   | 43              | 59   | 57   | 51              | 81   | 99   | 6                 | 7    | 9    |
| C2      | W      | 194  | 186  | 255  | 128             | 137  | 141  | 238             | 216  | 334  | 372             | 278  | 529  | 13                | 13   | 20   |
|         | S      | 73   | 60   | 124  | 48              | 43   | 67   | 89              | 70   | 144  | 173             | 106  | 266  | 11                | 19   | 12   |
|         | M      | 48   | 51   | 51   | 36              | 24   | 34   | 55              | 70   | 61   | 75              | 97   | 93   | 6                 | 12   | 12   |
| C3      | W      | 206  | 170  | 195  | 116             | 114  | 115  | 282             | 210  | 275  | 397             | 273  | 412  | 13                | 18   | 9    |
|         | S      | 85   | 87   | 125  | 50              | 58   | 79   | 118             | 110  | 139  | 170             | 158  | 239  | 12                | 17   | 15   |
|         | M      | 122  | 52   | 73   | 58              | 26   | 45   | 158             | 66   | 91   | 303             | 101  | 156  | 15                | 9    | 13   |
| C4      | W      | 208  | 135  | 242  | 143             | 81   | 141  | 272             | 198  | 304  | 389             | 237  | 509  | 14                | 16   | 11   |
|         | S      | 83   | 84   | 107  | 49              | 54   | 63   | 98              | 100  | 138  | 206             | 155  | 209  | 12                | 11   | 9    |
|         | M      | 100  | 47   | 162  | 66              | 15   | 89   | 110             | 61   | 209  | 176             | 87   | 455  | 7                 | 13   | 16   |
| C5      | W      | 206  | 136  | 196  | 125             | 82   | 125  | 271             | 191  | 298  | 398             | 253  | 505  | 11                | 7    | 16   |
|         | S      | 101  | 99   | 128  | 68              | 65   | 59   | 130             | 120  | 155  | 181             | 211  | 306  | 22                | 12   | 16   |
|         | M      | 61   | 57   | 193  | 49              | 12   | 97   | 67              | 65   | 283  | 109             | 136  | 402  | 9                 | 9    | 13   |
| C6      | W      | 194  | 151  | 329  | 143             | 93   | 192  | 222             | 215  | 428  | 325             | 216  | 629  | 8                 | 7    | 20   |
|         | S      | 82   | 83   | 126  | 37              | 53   | 82   | 99              | 90   | 144  | 228             | 163  | 263  | 12                | 8    | 11   |
|         | M      | 63   | 159  | 63   | 44              | 64   | 37   | 68              | 210  | 81   | 102             | 398  | 136  | 9                 | 23   | 9    |
| C7      | W      | 149  | 104  | 345  | 111             | 70   | 141  | 181             | 134  | 486  | 240             | 204  | 724  | 5                 | 14   | 9    |
|         | S      | 63   | 90   | 109  | 40              | 66   | 86   | 75              | 102  | 117  | 138             | 159  | 156  | 9                 | 8    | 10   |
|         | M      | 58   | 38   | 67   | 32              | 19   | 41   | 69              | 52   | 85   | 128             | 73   | 124  | 8                 | 11   | 10   |
| C8      | W      | 152  | 68   | 264  | 77              | 43   | 115  | 208             | 89   | 392  | 342             | 106  | 462  | 9                 | 5    | 3    |
|         | S      | 79   | 77   | 116  | 43              | 55   | 76   | 84              | 99   | 118  | 194             | 126  | 258  | 2                 | 5    | 6    |
|         | M      | 190  | 34   | 41   | 153             | 14   | 28   | 258             | 58   | 51   | 339             | 60   | 75   | 26                | 5    | 4    |
| C9      | W      | 198  | 64   | 170  | 122             | 55   | 121  | 254             | 72   | 373  | 366             | 97   | 478  | 12                | 5    | 5    |
|         | S      | 43   | 52   | 143  | 32              | 41   | 92   | 50              | 59   | 160  | 74              | 83   | 379  | 6                 | 4    | 11   |
|         | M      | 190  | 42   | 148  | 108             | 31   | 80   | 262             | 55   | 189  | 366             | 64   | 352  | 14                | 11   | 12   |



trajectories for 2008 and 2009) and C9 in 2010 (11% trajectories) originate from Arabian Sea and travel across Gujarat, Rajasthan, before arriving at the receptor site (Figure 3, Table 2). Shorter, moderately fast-moving trajectory cluster C6 (12%, 8%, and 11% trajectories in 2008, 2009, and 2010, respectively) originates from Gujarat in southwest and travels across Rajasthan, with significant dust loading from Rajasthan. About 35% of trajectories are clustered in short northwesterly flows (C1 and C5 in 2008, C1 and C2 in 2009, and C1, C3, and C4 in 2010) from Pakistan-Afghanistan region. These moderately fast airflows bend near Punjab above northwest of Delhi and have the highest loading of trajectories (Table 2). Short, slow-moving recirculating trajectory clusters around Delhi area constitute 20% of the trajectories in 2008 and 2010, and the remaining trajectories are from east and southeast in Uttar Pradesh (16%). Summer concentrations are lower than in winter. The shorter cluster C5 originating northwest on border from Pakistan has the highest mean value of  $100 \mu\text{g m}^{-3}$ , which is lower than mean values of aerosol concentrations connected with local and subregional cluster trajectories. The 95th percentile values of most of the clusters are quite high, ranging from 138 to  $220 \mu\text{g m}^{-3}$ , which reveal that irrespective of source of origin, the clusters eventually pick up local emissions around Delhi area. The interannual variability in summer transport patterns is negligible. The magnitude and range of  $\text{PM}_{2.5}$  concentrations are similar in 2008 and 2009. However, summer of 2010 has higher concentrations, since short, slow-moving trajectory clusters round the Delhi region and from neighboring Punjab and Haryana prevail and these have higher trajectory loading and higher concentrations (Table 2). The short recirculating trajectory cluster (C5) around Delhi in 2010 has the highest  $\text{PM}_{2.5}$  loading, with the highest average at  $128 \mu\text{g m}^{-3}$  and the highest 95th percentile distribution at  $306 \mu\text{g m}^{-3}$  (Table 2), showing the importance of subregional sources. Summer concentrations are much lower than winter concentrations, since in summer there is more vertical mixing and dispersal of pollutants.

*Monsoon season (2008–2010).*  $\text{PM}_{2.5}$  is characterized by low concentrations in monsoon due to removal by precipitation and wet deposition. The apparent seasonal patterns are similar to summer, with trajectory clusters distributed across northwest, west, southwest, southeast, and local circulating patterns (Figure 3). Short, slow-moving cluster C5 originating northwest of Delhi and C8 and C4 short recirculating clusters in 2008 and 2010, respectively, demonstrate the highest concentrations. The highest values for all the three years occur during postmonsoon period in the month of October, which also accounts for interannual variability in concentrations.

For all seasons, the dominant clusters are based on trajectory grouping originating from northwest and subregional recirculation wind patterns. The aerosol concentrations are also affected by transport from east of Delhi from urban regions of Uttar Pradesh. Overall, the trajectory cluster analysis at arrival height 500 m exhibits significant seasonal variability

but less interannual variability in the transportation pattern of trajectory, except in winter.

### Seasonal flow patterns at arrival height of 100 m and their allied concentrations

The sampling height of 100 m is chosen to distinguish more localized sources influencing the receptor site at Delhi. The cluster analysis discloses similar patterns of distinct seasonal flow patterns for all three seasons as 500 m altitude, revealing that dominating seasonal patterns are not so sensitive to arrival heights within the boundary layer. The altitude variation does impact the percentage of trajectories in each cluster, with percentage of trajectories much higher in local trajectory clusters rather than relatively long-distance clusters in comparison with 500 m arrival height.

The results show that the seasonal variability and interannual variability are consistent with the arrival heights at 500 m. The two sets of trajectory cluster analyses at 500 m and 100 m clearly display the predominance of regional industrial and urban sources mostly in the northwest in winter and recirculating, shorter clusters that indicate subregional sources on the borders of Delhi with adjacent states of Haryana and Uttar Pradesh.

### CWT method

The cluster analysis helps to demarcate the relative importance of regional source regions by quantifying differences between the clusters in terms of aerosol concentrations and the percentage of air masses present in each cluster. However, they are not completely effectual in determining relative contributions of potential source regions at the receptor site, which is accomplished by CWT approach that allocates concentrations to the relevant back trajectories at the receptor site and can distinguish between strong to moderate regional and subregional sources. Figure 4 demonstrates the distribution of weighted trajectory concentrations at 100 m arrival height for all seasons for representative year 2008. The CWT concentration gradients depict hotspots in winter, with highest potential contributions from subregional sources around the Delhi region and regional sources encompassing neighboring states of Punjab and Haryana in north, northwest, and urban regions of Uttar Pradesh towards northeast, east, and southeast. In case of winter, the highest concentrations at the receptor site from these sources are in the range of  $250 \mu\text{g m}^{-3}$  and above. In winter of 2009, this contribution drops to the range of  $200 \mu\text{g m}^{-3}$  and above, whereas in 2010 there are a larger number of grid cells providing above  $250 \mu\text{g m}^{-3}$  relative to 2008, with stronger potential emission inputs from subregional sources (figures not shown). Thus, from assessment of loading of the shorter, slower-moving clusters (Table 2) as they arrive at the receptor site and CWT analyses, we can put a guess estimate that sources located in neighboring states contribute 45–50% of cluster loading. Amongst long-distance sources, only industrialized regions on border of Punjab and Pakistan contribute above  $150 \mu\text{g m}^{-3}$  in CWT analyses, which is 15–20% of cluster loading originating from these regions that arrive at the receptor site.

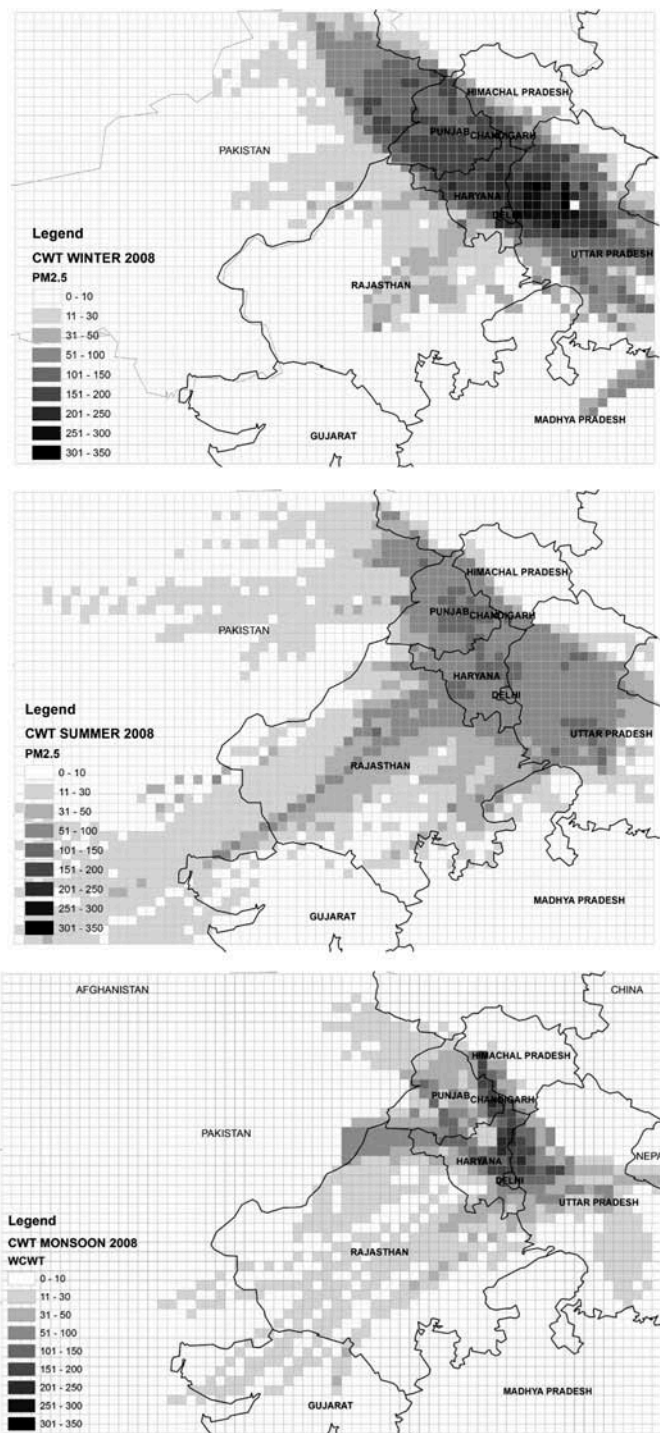


Figure 4. CWT plots for representative year 2008.

In summer, the southwest regions of Rajasthan and Gujarat are potential sources for all the three years, which contribute around 15% to total aerosol loading of the clusters that start from these regions. The immediate surrounding regions of Delhi and subregional sources have large contributions ranging mostly above 200  $\mu\text{g m}^{-3}$  for the three years. A few grid cells

surrounding Delhi contribute in excess of 200  $\mu\text{g m}^{-3}$ . During monsoon, the strongest concentration gradients are exhibited by regions immediately north and northwest of Delhi from the states of Haryana, Punjab, and subregional sources surrounding Delhi. The seasonal variations reveal the combined impact of back trajectories and pollutant concentrations. At 500 m arrival height, the CWT plots indicate similar concentration gradients as 100 m, but more widespread (figure not shown). All important potential source regions that cause accumulation of Delhi’s aerosol concentrations are covered by back trajectories arriving at 100 m arrival heights.

### Impact of emission sources on CWT concentrations

Since REAS version 2.1 emissions are available only for base year 2008, it has been considered a representative year in which total emissions and corresponding CWT values have been assembled across all grid cells for each of the three seasons at 0.25° grid resolution.

The total emissions for winter for year 2008 from all REAS emission source categories and from power plants are illustrated in Figure 5. There is not much seasonal variability in emission sources, and Figure 5 represents spatial distribution of emissions from other seasons as well. Intercomparison of CWT analyses in winter (Figure 4, top panel) with spatial distribution of emission sources (Figure 5) reveals strong correspondence of potential regions of high source concentrations to significant emissions. Overall values of Pearson’s correlation coefficients between emissions and CWT concentrations in corresponding grid cells are 0.56 in winter, 0.45 in monsoon, and 0.28 in summer. A statistical measure, gamma ( $\gamma$ ), used to depict degree of association between different categories (from low to high) of total seasonal emissions and CWT concentrations, reveals that  $\gamma$ -values are highest in winter (0.83), followed by monsoon (0.57) and then summer (0.38). The results depicted in Table 3 reveal that in winter, 87% of high CWT values between 75th and 90th percentiles and 89% of CWT concentrations above 90th percentile are associated with high ranges of emissions sources (75th percentile and above). In summer, higher CWT concentrations are linked more with nonsource regions, showing effects of increased mixing and dispersion of emissions downwind. The results substantiate the fact that in winter, emission source regions contribute more directly to trajectory residence time weighted concentrations in the allied grid cells on account of poor dispersion of emissions due to surface inversion and lower mixing heights than other seasons. Emissions from power plants and industries within Delhi City itself and the border of Delhi with states of Uttar Pradesh, Punjab, and Haryana are major sources of regional  $\text{PM}_{2.5}$  concentrations over Delhi. Most of these thermal power plants are coal-based and are key emitters of  $\text{PM}_{2.5}$ . The domestic regional sources include biomass, coal, and wood burning in winter, and other low point sources such as cement industries and brick kilns, or nonpoint sources such as extensive zones of construction activities, which are major emitters of  $\text{PM}_{2.5}$ . Amongst distant sources, only hotspots on border of Punjab and Pakistan (Figure 5) may contribute to Delhi’s emissions, substantiated by trajectory clustering and CWT analyses.

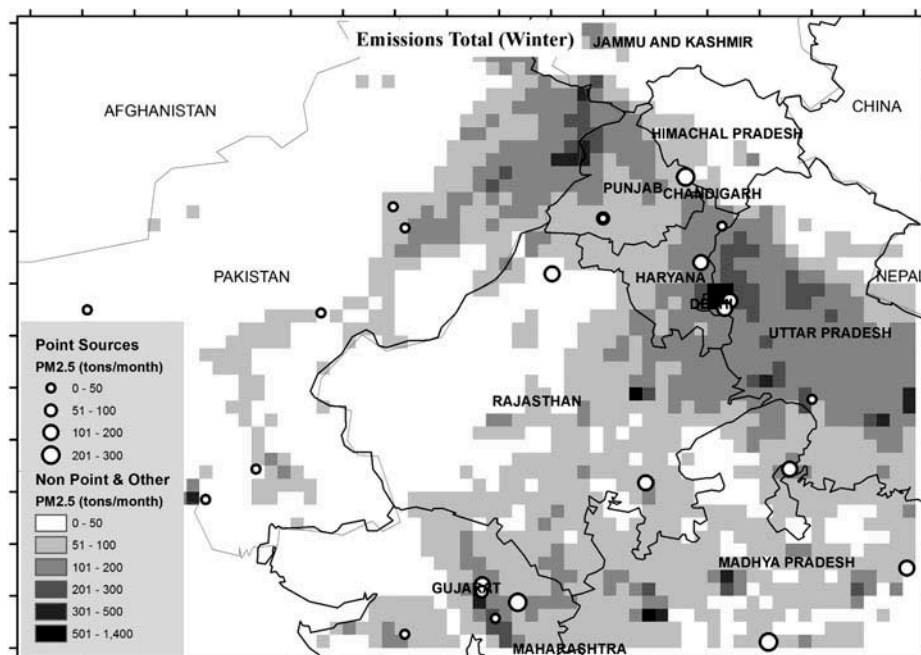


Figure 5. Total emissions in winter of 2008, with power plants superimposed on grid cells.

Table 3. Percentage of major source areas associated with different ranges of emissions

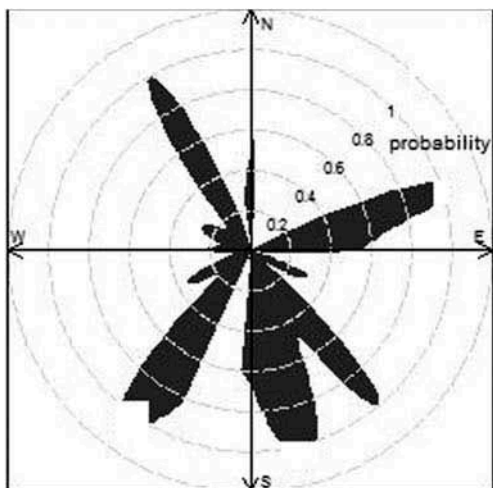
| Emission (percentile) | Percentage of CWT Concentrations<br>75th–90th Percentiles |        |         | Percentage of CWT Concentrations<br>>90th Percentiles |        |         |
|-----------------------|---|--------|---------|---|--------|---------|
|                       | Winter  | Summer | Monsoon | Winter  | Summer | Monsoon |
| 0–25                  | 1   | 23     | 4       | 6   | 22     | 4       |
| 25–75                 | 12  | 67     | 18      | 5   | 63     | 6       |
| 75–90                 | 58  | 6      | 43      | 45  | 10     | 45      |
| >90                   | 29  | 4      | 35      | 44  | 5      | 44      |

### Local sources and their contribution

Wind direction and wind speed from Delhi Airport for three consecutive years and for all seasons have been used to identify local sources. Conditional probability function of elevated  $PM_{2.5}$  concentrations (seasonal 75th percentile) associated with prevailing wind directions has been represented in Figure 6. In winter, maximum contributions from local sources are in the southwest and southeast directions, with lesser contributions from local sources in northwest and northeast. In summer, greater contributions are from the northeast for the 75th percentile concentrations and in monsoon from northwest and southeast. The industrial and commercial satellite towns of Noida (southeast), Faridabad (south), and Gurgaon (south-southwest) are located in the arc covering southwest to southeast of Delhi. Clusters of industries such as smelters, tanneries, textiles, manufacturing, chemicals, paper, and pharmaceuticals operate in Faridabad and Gurgaon (in the southern sector), Ghaziabad (in the east), and Janakpuri (in the west), from where local

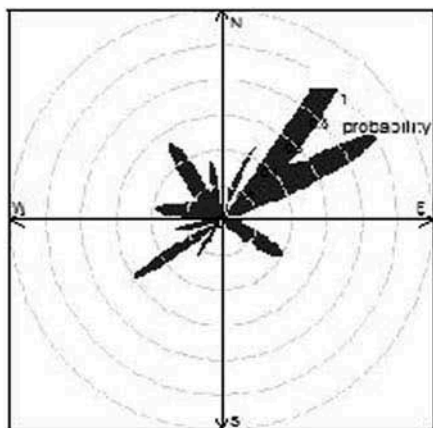
emissions emanate. Most of these urban regions located in other states form a part of National Capital Territory (NCR). Detailed emission inventory for Delhi and surrounding NCR region are presented in the paper by Guttikunda and Calori (2013). These results are also borne out by trajectory clustering approach where short clusters from these directions have the highest distribution of concentrations (Table 2), indicating that regional trajectories pick up emissions from these areas while approaching the ITO site.

Using the Bayesian approach to summarize prevailing wind directions in case of high  $PM_{2.5}$  concentrations (daily averages exceeding  $120 \mu g m^{-3}$ ), it is seen from Table 4 that contribution of sources located in the arc encompassing southwest-south (more than 22%) and south-southeast (more than 40%) are the most towards  $PM_{2.5}$  concentrations, above  $120 \mu g m^{-3}$ , since these wind directions prevail in winter where more number of values exist in this range than other seasons. The southwest and southeast sectors consist of highly urbanized townships of the Delhi NCR region as mentioned above.



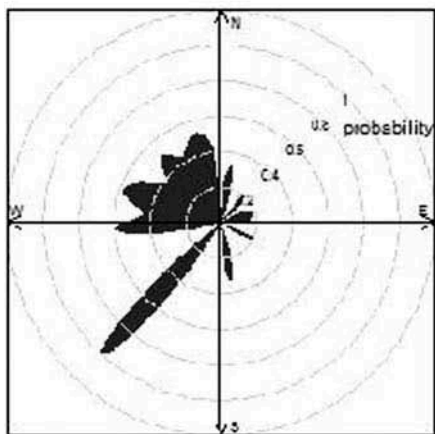
CPF at the 75th percentile (=249.9)

(a) Winter, 2008-2010



CPF at the 75th percentile (=120)

(b) Summer, 2008-2010



CPF at the 75th percentile (=99.9)

(c) Monsoon, 2008-2010

Figure 6. Conditional probability function of high PM<sub>2.5</sub> concentrations for different wind directions (2008–2010).

Table 4. Contribution of each direction towards high value of PM<sub>2.5</sub> (>120 μg m<sup>-3</sup>)

| Season  | E-NE<br>0°–45° | NE-N<br>45°–90° | N-NW<br>90°–135° | NW-W<br>135°–180° | W-SW<br>180°–225° | SW-S<br>225°–270° | S-SE<br>270°–315° | SE-E<br>315°–360° |
|---------|----------------|-----------------|------------------|-------------------|-------------------|-------------------|-------------------|-------------------|
| Winter  | 0.03           | 0.04            | 0.09             | 0.06              | 0.01              | 0.31              | 0.42              | 0.04              |
| Summer  | 0.07           | 0.05            | 0.14             | 0                 | 0.01              | 0.21              | 0.42              | 0.10              |
| Monsoon | 0.02           | 0.06            | 0.09             | 0                 | 0.02              | 0.26              | 0.45              | 0.10              |

## Conclusion

The study demonstrates simulated trajectories from north-west exhibit high PM<sub>2.5</sub> concentrations during all seasons but especially during winter for all the three years 2008–2010. Regional, slower-moving clusters from Afghanistan and urban regions in Pakistan in northwest direction enhance cluster loading by picking up emissions as they traverse over highly urbanized regions in Punjab and Haryana as they travel to the receptor site. Long-distance fast trajectory clusters north-west from relatively clean source regions in Iran, Iraq, Russia, and Saudi Arabia do not have much impact on PM<sub>2.5</sub> concentrations due to shorter residence times as they cross emission rich areas. The dominant regional PM<sub>2.5</sub> sources from the northwest urban regions are power plants, industrial clusters, and other domestic sources such as biomass, coal, and wood burning in winter. Recirculating shorter, slow-moving trajectories in winter pick up PM<sub>2.5</sub> concentrations possibly from coal-based thermal power plants and industrial plumes in Punjab (Ropar), Haryana, and Uttar Pradesh and further collect PM<sub>2.5</sub> concentrations locally within Delhi before they reach the ITO site. The cluster analysis reveals dust loading possibly from Thar Desert in Rajasthan region, especially in summer. Conditional probability function and Bayesian approach identify dominant local sources around Delhi, especially on an arc from southeast to southwest of Delhi comprising highly urbanized satellite towns located in NCR region such as Noida, Faridabad, and Gurgaon (contributions around 70%). Elevated source regions from REAS emission inventory substantiate significant potential regional source contributions identified by CWT analyses situated in neighboring states of Punjab, Haryana, and Uttar Pradesh. The analyses reveal that high emissions in Delhi-NCR region and its immediate surroundings states are responsible for the high PM<sub>2.5</sub> concentrations, which substantially exceed NAAQS standards (60 µg m<sup>-3</sup>) for all the three years. The daily PM<sub>2.5</sub> concentrations and variability are highest in winter of 2010. The year 2009 has the lowest winter concentrations and variability. There is considerable seasonal variability, with maximum concentrations in winter and changes in trajectory cluster patterns between winter, summer, and monsoon seasons. There is less interannual variability of trajectory cluster patterns in case of summer and monsoon. This study reveals that seasonal and annual fluctuations in aerosol concentrations are caused by meteorological variability. Stringent emission reduction strategies need to be developed that must account for changes in air circulation patterns and associated transboundary flux to counter nonlinear seasonal and interannual variations in PM<sub>2.5</sub> concentrations to provide a remedial solution to Delhi's air quality problem.

## References

Biswas, J., E. Upadhyay, M. Nayak, and A.K. Yadav. 2011. An analysis of ambient air quality conditions over Delhi, India from 2004 to 2009. *Atmos. Clim. Sci.* 1:214–224. doi:10.4236/acs.2011.14024

Budhavant, K.B., P.S.P. Rao, P.D. Safai, L. Granat, and H. Rodhe. 2014. Chemical composition of the inorganic fraction of cloud-water at a high

altitude station in West India. *Atmos. Environ.* 88:59–65. doi:10.1016/j.atmosenv.2014.01.039

Buseck, P.R., and S.E. Schwartz. 2014. Tropospheric aerosols, reference module in earth systems and environmental sciences from *Treatise on Geochemistry (2nd ed.)*. *The Atmosphere* 5:95–137.

Carlsaw, D.C., and K. Ropkins. 2012. An open air R package for air quality data analysis. *Environ. Modell. Softw.* 27–28:52–61.

Cheng, I., L. Zhang, P. Blanchard, J. Dalziel, and R. Tordon. 2013. Concentration-weighted trajectory approach to identifying potential sources of speciated atmospheric mercury at an urban coastal site in Nova Scotia, Canada. *Atmos. Chem. Phys.* 13:6031–6048. doi:10.5194/acp-13-6031-2013

Chuang, M.-T., C.-T. Lee, C.C.-K. Chou, N.-H. Lin, G.-R. Sheu, J.-L. Wang, S.-C. Chang, S.-H. Wang, K.H. Chi, C.-Y. Young, et al. 2014. Carbonaceous aerosols in the air masses transported from Indochina to Taiwan. Long-term observation at Mt. Lulin. *Atmos. Environ.* 89: 507–516. doi:10.1016/j.atmosenv.2013.11.066

Central Pollution Control Board (CPCB). 2014. Continuous ambient air quality. <http://cpcb.nic.in> (accessed May 14, 2014).

Daniel, W.W. 1979. *Applied Nonparametric Statistics*. Boston: Houghton Mifflin.

Dholakia, H.H., P. Purohit, S. Rao, and A. Garg. 2013. Impact of current policies on future air quality and health outcomes in Delhi, India. *Atmos. Environ.* 75:241–248. doi:10.1016/j.atmosenv.2013.04.052

Draxler, R.R., and G.D. Hess 1998. An overview of the HYSPLIT\_4 modeling system of trajectories, dispersion, and deposition. *Aust. Meteorol. Mag.* 47:295–308.

Gogoi, M.M., B. Pathak, K. Krishna Moorthy, P.K. Bhuyan, S. Suresh Babu, K. Bhuyan, and G. Kalita. 2010. Multi-year investigations of near-surface and columnar aerosols over Dibrugarh, North-eastern location of India: Heterogeneity in source impacts. *Atmos. Environ.* 45:1714–1724.

Gupta, M., and M. Mohan. 2013. Assessment of contribution to PM<sub>10</sub> concentrations from long range transport of pollutants using WRF/Chem over a subtropical urban airshed. *Atmos. Pollut. Res.* 4:405–410. doi:10.5094/APR.2013.046

Gupta, S., S. Venkataramani, Y.B. Acharya, and S. Lalm. 2006. Vertical distribution of ozone over the Bay of Bengal and the Arabian Sea during ICARB campaign. In *Proceedings of First Post Campaign meeting of ICARB, October 25–27, 2006, Space Physics Laboratory, Trivandrum*.

Gurjar, B.R., J.A. van Aardenne, J. Leliveld, and M. Mohan. 2005. Emission estimates and trends (1990–2000) for megacity Delhi and implications. *Atmos. Environ.* 38:5663–5681. doi:10.1016/j.atmosenv.2004.05.057

Guttikunda, S.K. 2009. Air quality management in Delhi, India: Then, now and next. In *SIM-Air Working Paper Series 22, UrbanEmissions.Info*, 1–8. <http://www.sim-air.org/> (accessed November 12, 2014).

Guttikunda, S., and B. Gurjar. 2012. Role of meteorology in seasonality of air pollution in megacity Delhi, India. *Environ. Monit. Assess.* 184:3199–3211.

Guttikunda, S.K., and G. Calori. 2013. A GIS based emissions inventory at 1 km × 1 km spatial resolution for air pollution analysis in Delhi, India. *Atmos. Environ.* 67:101–111. doi:10.1016/j.atmosenv.2012.10.040

Guttikunda, S.K., and R. Goel. 2013. Health impacts of particulate pollution in a megacity—Delhi, India. *Environ. Dev.* 6:8–20. doi:10.1016/j.envdev.2012.12.002

Guttikunda, S.K., and B.R. Gurjar. 2012. Role of meteorology in seasonality of air pollution in megacity Delhi, India. *Environ. Monit. Assess.* 184: 3199–3211. doi:10.1007/s10661-011-2182-8

Han, Y.J., T. M. Holsen, and P.K. Hopke. 2007. Estimation of source locations of total gaseous mercury measured in New York State using trajectory-based models. *Atmos. Environ.* 41:6033–6047. doi:10.1016/j.atmosenv.2007.03.027

Health Effects Institute. 2010a. *Traffic-Related Air Pollution. A Critical Review of the Literature of Emissions, Exposure, and Health Effects*. Special Report 17. Boston: Health Effects Institute.

Health Effects Institute. 2010b. *Outdoor Air Pollution and Health in the Developing Countries of Asia: A Comprehensive Review*. Special Report 18. Boston: Health Effects Institute.

- Khaiwal, R., E. Wauters, S. Tyagi, M. Suman, and R.V. Grieken. 2006. Assessment of air quality after the implementation of Compressed Natural Gas (CNG) as fuel in public transport in Delhi, India, 2006. *Environ. Monit. Assess.* 115:405–417.
- Ketzel, M., and R. Berkowicz. 2005. Multi-plume aerosol dynamics and transport model for urban scale particle pollution. *Atmos. Environ.* 39: 3407–3420. doi:10.1016/j.atmosenv.2005.01.058
- Krakow, J., T. Ohara, T. Morikawa, S. Hanayama, J.M. Greet, T. Fukuil, K. Kawashima, and H. Akimoto. 2013. Emissions of air pollutants and greenhouse gases over Asian regions during 2000–2008: Regional Emission inventory in Asia (REAS) version 2. *Atmos. Chem. Phys. Discuss.* 13:10049–10123.
- Kurokawa, J., and T. Ohara. 2014. Trends of anthropogenic emissions of air pollutants over Southeast and South Asia. *International Workshop on Air Quality in Asia, Hanoi, Vietnam, June 24–26.*
- Li, J., G. Wang, S.G. Aggarwal, Y. Huang, Y. Ren, B. Zhou, K. Singh, P.K. Gupta, J. Cao, and R. Zhang. 2014. Comparison of abundances, compositions and sources of elements, inorganic ions and organic compounds in atmospheric aerosols compositions from Xi'an and New Delhi, two megacities in China and India. *Sci. Total Environ.* 476–477:485–495.
- Liu, N., Y. Yu, J. He, and S. Zhao. 2013. Integrated modeling of urban-scale pollutant transport: Application in a semi-arid urban valley, Northwestern China. *Atmos. Pollut. Res.* 4:306–314. doi:10.5094/APR.2013.034
- Markou, M.T., and P. Kassomenos. 2010. Cluster analysis of five years of back trajectories arriving in Athens, Greece. *Atmos. Res.* 98:438–457. doi:10.1016/j.atmosres.2010.08.006
- Miller L., S. Farhana, and X. Xu. 2010. Trans-boundary air pollution in Windsor, Ontario (Canada). *Procedia Environ. Sci.* 2:585–594.
- Mitra, A. P., and C. Sharma. 2002. Indian aerosols: Present status. *Chemosphere* 49:1175–1190. doi:10.1016/S0045-6535(02)00247-3
- Mohan, M., and S. Payra. 2009. Influence of aerosol spectrum and air pollutants on fog formation in urban environment of megacity Delhi, India. *Environ. Monit. Assess.* 151:265–277. doi:10.1007/s10661-008-0268-8
- National Research Council. 2010. *Global Sources of Local Pollution.* Washington, DC: National Academy of Sciences.
- Norman, M., S.N. Das, A.G. Pillai, L. Granat, and H. Rodhe. 2001. Influence of air mass trajectories on the chemical composition of precipitation in India. *Atmos. Environ.* 35:4223–4235. doi:10.1016/S1352-2310(01)00251-5
- O'Connor, T.C., S.G. Jennings, and C.D. O'Dowd. 2008. Highlights of fifty years of atmospheric aerosol research at Mace Head. *Atmos. Res.* 90: 338–355. doi:10.1016/j.atmosres.2008.08.014
- Ohara, T., H. Akimoto, J. Kurokawa, N. Horii, K. Yamaj, X. Yan, and T. Hayasaka. 2007. An Asian emission inventory of anthropogenic emission sources for the period 1980–2020. *Atmos. Chem. Phys.* 7: 4419–4444. doi:10.5194/acp-7-4419-2007
- Pandey, J. S., K. Rakesh, and S. Devotta. 2005. Health Risks of NO<sub>2</sub>, SPM and SO<sub>2</sub> in Delhi (India). *Atmos. Environ.* 39:6868–6874. doi:10.1016/j.atmosenv.2005.08.004
- Pope, C.A., III, R. Brook, R. Burnett, and D. Dockery. 2011. How is cardiovascular disease mortality risk affected by duration and intensity of fine particulate matter exposure? An integration of the epidemiologic evidence. *Air Qual. Atmos. Health* 4(1):5–14. doi:10.1007/s11869-010-0082-7
- Rana, S., Y. Kant, and V.K. Dadhwal. 2009. Diurnal and seasonal variation of spectral properties of aerosols over Dehradun, India. *Aerosol Air Qual. Res.* 9:32–39. doi:10.4209/aaqr.2008.06.0019
- Salvador, P., B. Artinano, X. Querol, and A. Alastuey. 2008. A combined analysis of backward trajectories and aerosol chemistry to characterise long-range transport episodes of particulate matter: The Madrid air basin, a case study. *Sci. Total Environ.* 390:495–506. doi:10.1016/j.scitotenv.2007.10.052
- Sharma, P., P. Sharma, S. Jain, and P. Kumar. 2013. An integrated statistical approach for evaluating the exceedance of criteria pollutants in the ambient air of megacity Delhi. *Atmos. Environ.* 70:7–17. doi:10.1016/j.atmosenv.2013.01.004
- Shindell, D., and G. Faluvegi. 2009. Climate response to regional radiative forcing during the twentieth century. *Nat. Geosci.* 2:294–300. doi:10.1038/ngeo473
- Shindell, D., J.C.I. Kuylenstierna, E. Vignati, R.V. Dingenen, M. Amann, Z. Klimont, S.C. Anenberg, N. Muller, G.J.-Maenhout, F. Raes, et al. 2012. Simultaneously mitigating near-term climate change and improving human health and food security. *Science* 335: 183–189. doi:10.1126/science.1210026
- Singh, D.P., R. Gadi, and T.K. Mandal. 2011. Characterization of particulate-bound polycyclic aromatic hydrocarbons and trace metals composition of urban air in Delhi, India. *Atmos. Environ.* 40:7653–7663. doi:10.1016/j.atmosenv.2011.02.058
- Srivastava, A., and V. K., Jain. 2007. Seasonal trends in coarse and fine particle sources in Delhi by the chemical mass balance receptor model. *J. Hazard. Mater.* 144:283–291. doi:10.1016/j.jhazmat.2006.10.030
- Srivastava, A.K., S. Singh, S. Tiwari, V.P. Kanawade, and D.S. Bisht. 2012. Variation between near-surface and columnar aerosol characteristics during the winter and summer at Delhi in the Indo-Gangetic Basin. *J. Atmos. Solar Terr. Phys.* 77:57–66. doi:10.1016/j.jastp.2011.11.009
- Stohl, A., S. Eckhardt, C. Forster, P. James, N. Spichtinger, and P. Seibert. 2002. A replacement for simple back trajectory calculations in the interpretation of atmospheric trace substance measurements. *Atmos. Environ.* 36:4635–4648. doi:10.1016/S1352-2310(02)00416-8
- Tiwari, S., A.K. Srivastava, D.S. Bisht, P. Parmita, M. K. Srivastava, and S.D. Attri. 2013. Diurnal and seasonal variations of black carbon and PM<sub>2.5</sub> over New Delhi, India: Influence of meteorology. *Atmos. Res.* 125–126:50–62. doi:10.1016/j.atmosres.2013.01.011
- Wang, Y.Q., X.Y. Zhang, and R.R. Draxler. 2009. TrajStat: GIS-based software that uses various trajectory statistical analysis methods to identify potential sources from long-term air pollution measurement data. *Environ. Modell. Softw.* 24:938–939. doi:10.1016/j.envsoft.2009.01.004
- Zhang, K. M., and A. S. Wexler. 2008. Modeling urban and regional aerosols—Development of the UCD aerosol module and implementation in CMAQ model. *Atmos. Environ.* 42:3166–3178. doi:10.1016/j.atmosenv.2007.12.052

## About the Authors

**Saikat Ghosh** is an air quality modeling specialist at Air Quality Centre at Ohio University, Athens, OH, USA.

**Jhmoor Biswas** is currently associate professor in the Department of Environmental Management, Indian Institute of Social Welfare and Business Management, Kolkata, Indian.

**Sarath Guttikunda** is a TED Fellow and an affiliate associate professor at Desert Research Institute in Reno, NV, USA and is the director of an independent research group UrbanEmissions.Info (UEinfo, India).

**Soma Roychowdhury** is a professor of statistics at Indian Institute of Social Welfare and Business Management, Calcutta, India and a visiting professor of Statistics at the University of California, Davis, USA.

**Mugdha Nayak** is an assistant professor at Ansal Institute of Technology, Gurgaon, India.